2020: The Journal of Astronomical Data 26, 1.

CCD photometry of CY Aquarii VI.
The 2019–2020 seasons

C. Wiedemair[1], C. Sterken[2], T. Eenmäe[3], R. Neito[3],
V. Oberhauser[1], D. Moser[1], M. Mair[1], and G. Lercher[1]
[1] Cusanus-Gymnasium Bruneck, 39031 Bruneck, Italy
[2] Vrije Universiteit Brussel, 1050 Brussels, Belgium
[3] Tartu Observatory, University of Tartu, 61602 Tõravere, Estonia

Received November 22, 2020, accepted December 3, 2020

Abstract

Based on 28 partial nights of CCD monitoring, we derive 49 new times of maximum light of the SX Phoenicis star CY Aquarii. These times extend the linear ephemeris for a time interval covering the last eight years.

Keywords: technique: photometric – stars: individual: CY Aqr – variable stars: SX Phoenicis stars – variable stars: period change

1 Introduction

CY Aquarii (BD +00°4900) is a short-period ($P = 87.9$ min), large-amplitude ($0\overset{\mathrm{m}}{.}71$ in V) SX Phoenicis star. Since the discovery of its variability in 1934, this pulsating star has been extensively observed, and several investigations of its changing pulsation period, using the $O-C$ diagram, have been published since the 1950s.

The latest deep studies on the period change of CY Aqr were by Fu & Sterken (2003) and by Fang *et al.* (2016). Invoking a linear period change combined with the light-time effect in a highly-eccentric orbit, Fu & Sterken (2003) presented one possible solution invoking a binary with eccentricity $e = 0.77 \pm 0.01$ and orbital period $P_{\mathrm{orb}} = 52.5 \pm 0.3$ years. Fang *et al.* (2016) analyzed maxima collected from the literature, and provided a revised period and a new ephemeris. These authors conclude that CY Aqr is very probably a triple system with two low-mass companions with periods 54.2 and 47.3 years in an eccentric orbit.

This is our sixth data paper presenting a set of new times of maximum of CY Aqr. Previous papers are Tuvikene *et al.* (2010) [Paper I], Sterken *et al.* (2011, 2012) [Paper

II, III] and Wiedemair *et al.* (2016, 2018) [Paper IV, V]. The present paper gives a set of over 9 700 differential magnitudes and 49 new timings obtained in 2019–2020. These times extend the linear ephemeris of Paper V over a time interval covering the last eight years.

The aim of this paper is not to derive a new model to explain the complicated behavior of this star, but to provide a growing set of accurate timings obtained in consecutive observing seasons in order to follow the period variation of this system at high time resolution. No conclusions on the physical origin of the period changes are attempted, but the resulting linear ephemeris formulae are used to delineate time intervals during which the period can be considered constant (within the given statistical bounds) and will serve for planning future observations. Our new data are set in the framework of the model by Fu & Sterken (2003) that incorporates almost all the times of maximum that had been previously determined.

2 Observations

All photometric data reported in this paper were obtained through CCD imaging on 28 partial nights, and comprise a total of over 9 500 useful CCD frames. Table 1 gives the journal of observations. Figure 1 is a $18' \times 12'$ sky map of CY Aqr and its neighboring comparison stars.

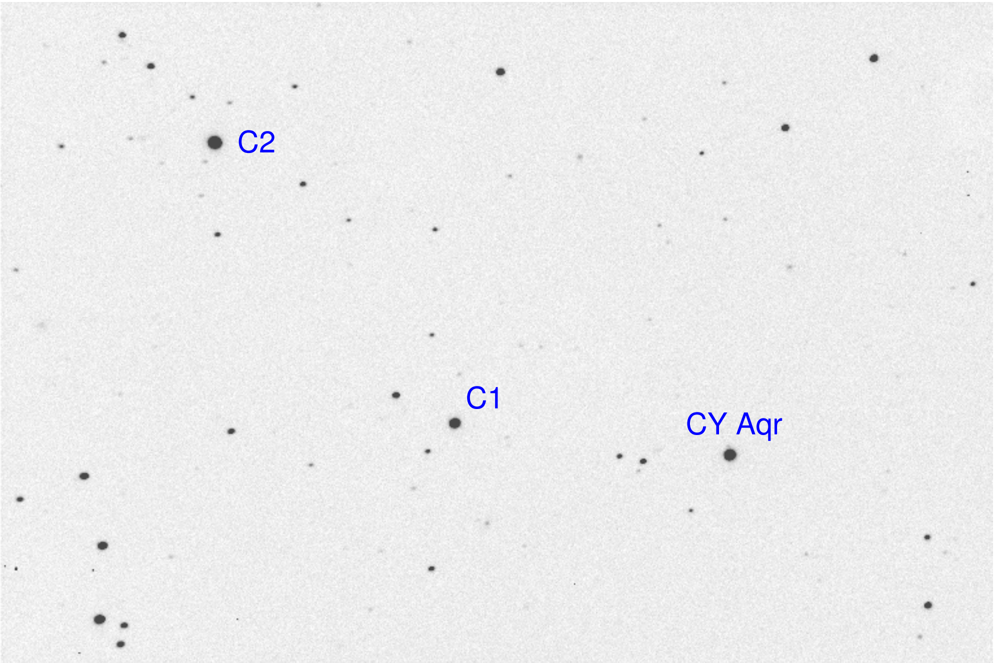

Figure 1: CY Aqr CCD field, from Sterken *et al.* (2011). North is up and East is left, field of view is $18' \times 12'$. CY Aqr and the comparison stars C_1 = GSC 00567–01826 and C_2 = GSC 00567–02036 are marked.

2.1 Observations at the Nikolaus Cusanus Gymnasium Bruneck

The observations were obtained from a roll-off-roof observatory located at a 1600-m altitude site near Bruneck (Südtirol, Italy), by C. Wiedemair and a team of students. A 16-inch Ritchey-Chretien $f/8$ telescope with a SBIG ST8-XME CCD camera was used. Exposure time was 12 s, with 2×2 binning, and no filter was used. Flat-field frames were obtained by taking 6-second exposures of a light foil placed in front of the telescope aperture. Data frames were calibrated with nightly-averaged master darks and flats.

2.2 Observations at Tartu Observatory

At Tartu Observatory, a 0.6-m $f/12.5$ Cassegrain Zeiss 600 reflector was used. This telescope is equipped with an Andor Ikon-L CCD camera with a Johnson V-band Optec Inc glass photometric filter. Most of the observations were done in full resolution of the CCD sensor using 30-second exposures, except during some nights in 2020 when 2×2 binning was applied. Binning allowed to improve the observing cadence by approximately a factor of two at 15-second exposure times. Bias frames and twilight sky flat field frames were used for calibration. Because the camera is cooled to $-75°$ C, no dark frames were needed.

3 Data reduction

All observations were reduced by T. Eenmäe using routines of the IDL Astronomy User's Library[1] in a workflow as described by Tuvikene (2012). Aperture size was scaled with the full width at half maximum (FWHM) of the stellar image, and an aperture radius of $1.6\times$ FWHM was used for all frames, see also Tuvikene & Sterken (2010). For reasons of verification, magnitudes of the Bruneck CCD frames were extracted by C. Wiedemair by means of aperture photometry as implemented in the `Muniwin`[2] reduction package.[3]

The data in this paper are differential light curves relative to C_1 = GSC 00567–01826 as comparison star. Differential magnitudes of the comparison stars are also given to assess the precision of our data. The average differential magnitude of the comparison stars is listed in Table 2. Poor nights, and outliers, were removed using these differential magnitude curves.

All differential magnitudes of CY Aqr and of the two comparison stars are given in online Tables `2019-2020bruneck.dat` and `2019-2020-tartu.dat`.

4 The times of maximum

Times of maximum light were determined from visual inspection of the light curves within $\pm 0\overset{\mathrm{d}}{.}005$ of the moment of maximum light, supported by a moving-average line. From multiple readings of the same sections of light curves, we estimate that the internal precision of one single time of maximum as derived via our approach is $0\overset{\mathrm{d}}{.}00003$ (< 3 sec). The accuracy

---

[1] `idlastro.gsfc.nasa.gov`

[2] `http://c-munipack.sourceforge.net`

[3] The image calibration for this verification run was done with `Pixinsight` (`pixinsight.com/`).

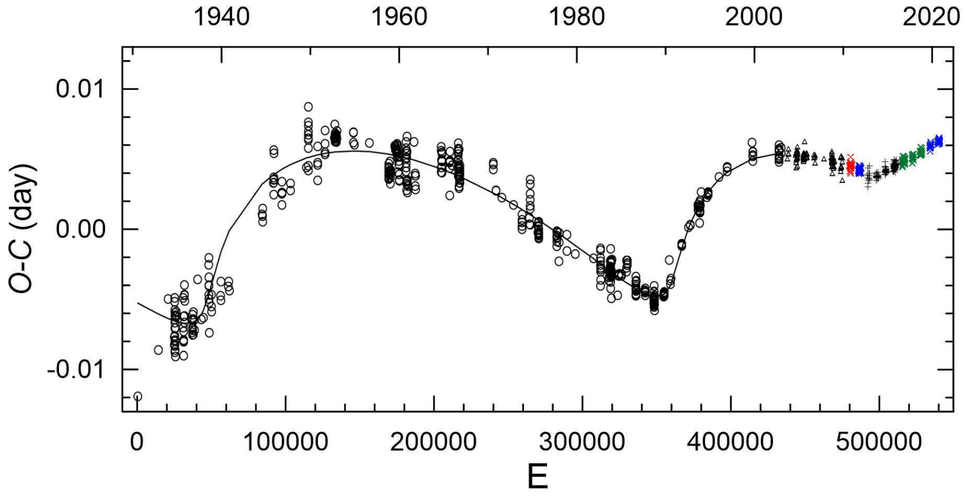

Figure 2: $O-C$ curve from Fu & Sterken (2003). Full line and ○: light-time orbit solution and data from Fu & Sterken (2003); △, black: $+$: Paper I; $\times$, red color: Paper II; $\times$, blue color: Paper III; $+$, black: Paper IV; $\times$, green color: Paper V; $\times$, blue color: all $T_{\max}$ listed in this paper.

of a timing can be best estimated from the three cycles that were simultaneously observed in Bruneck and in Tartu, which indicate that differences between the estimated times of maximum can amount to $0^{\mathrm{d}}.0002$. Relative weights have been assigned using the same criteria as used in Tuvikene *et al.* (2010), see Table 3. Table 4 (online file `tmax2019-20.dat`) lists the results, with corresponding weight factors and cycle number E.

5 Ephemeris and resulting *O–C* diagrams

Paper V used 168 maxima to derive a linear ephemeris for 2013–2018 that yielded $P = 0.061038428 \pm 0.000000002$. Our new data lead to essentially the same ephemeris for 2013–2020, though with slightly improved accuracy:

$$\begin{array}{rcccc} T_{\max} & = & 2426159.47142 & + & 0.061038430\,E \\ & & \pm 0.00001 & & \pm 0.000000001 \end{array} \qquad (1)$$

6 Discussion

Figure 2 shows the new $O-C$ points overplotted in Fig. 3 of Fu & Sterken (2003, ephemeris $T_{\max} = 2426159.4967 + 0.0610383716E$) together with $O-C$ values of Papers II–V, and of the present paper.

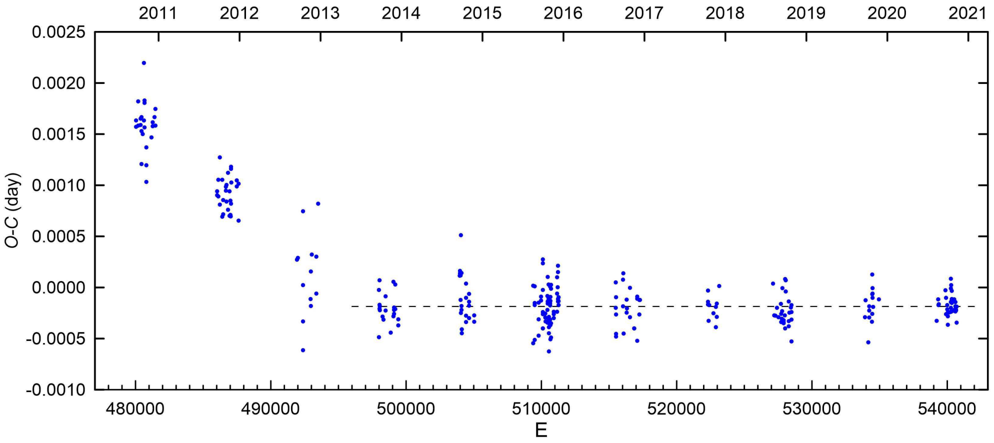

Figure 3: $O-C$ values calculated with ephemeris (2). The dashed line represents the current constant period $P = 0\overset{\text{d}}{.}061038430 \pm 0\overset{\text{d}}{.}000000001$.

The average $O-C$ with respect to Eq. (2) amounts to 0.00012 with standard deviation $\sigma = 0.00006$ for the entire time interval 2013–2020. As indicated in Papers IV and V, the pulsation period most likely changed shortly before or around 2013, but neither the onset of the change nor the duration (i.e., the "suddenness" of the period change) was captured. Figure 3 illustrates the period change, as well as the higher variance of the 2012 $O-C$ values that is about twice as high as the variance in the subsequent years 2013–2020.

7 Conclusion

While the data presented in this paper support a stationary period during the last eight years, our new data set provides increasing evidence that a physical model of CY Aqr in terms of multiple stellar companions becomes hard to maintain.

Acknowledgments

This paper is based on observations made at the Cusanus-Gymnasium Bruneck, Italy (formerly Realgymnasium Bruneck) and observations made at the Tartu Observatory, Estonia.

This work was supported by the institutional research funding IUT40-1 of the Estonian Ministry of Education and Research. The work at the Cusanusgymnasium Bruneck benefits from the ongoing support of "Deutsche Bildungsdirektion", Südtirol, Italy.
This research has made use of the SIMBAD and NASA ADS data bases.

References

Fang, Wei-Jing, Luo, Zhi-Quan, Zhang, Xiao-Bin et al. 2016, Research in Astronomy and Astrophysics, Volume 16, Issue 6, article id. 96

Fu, J. N. & Sterken, C. 2003, A&A, 405, 685

Sterken, C., Wiedemair, C., Tuvikene, T. *et al.* 2011, JAD, 17, 2 (paper II)

Sterken, C., Wiedemair, C., Munaro, T. *et al.* 2012, JAD, 18, 2 (paper III)

Tuvikene, T. & Sterken, C. 2010, JAD, 16, 1

Tuvikene, T., Sterken, C., Brogt, E. *et al.* 2010, JAD, 16, 2 (paper I)

Tuvikene, T. 2012, PhD thesis, Vrije Universiteit Brussel

Wiedemair, C., Sterken, C., Tuvikene, T. *et al.* 2016, JAD, 22, 1 (paper IV)

Wiedemair, C., Sterken, C., Eenmäe, T. *et al.* 2018, JAD, 24, 4 (paper V)

Table 1: Journal of observations: JD, number of CCD frames, average differential magnitude between comparison stars, and standard deviation σ for each nightly sequence.

JD−2400000	N	$C_1 - C_2$	σ	Band	Site
58749.38 – .44	152	−1.021	0.005	V	Tartu 2019
58752.36 – .42	151	−1.022	0.005	V	Tartu 2019
58764.40 – .43	71	−1.021	0.006	V	Tartu 2019
58768.26 – .41	721	−1.036	0.009	–	Bruneck 2019
58780.35 – .37	87	−1.032	0.012	–	Bruneck 2019
58782.39 – .37	899	−1.035	0.010	–	Bruneck 2019
58783.27 – .43	984	−1.034	0.009	–	Bruneck 2019
58786.39 – .44	127	−1.033	0.010	V	Tartu 2019
58787.35 – .38	54	−1.023	0.007	V	Tartu 2019
58812.25 – .38	129	−1.094	0.008	V	Tartu 2019
59072.41 – .45	96	−1.038	0.004	V	Tartu 2020
59079.38 – .41	71	−1.039	0.007	V	Tartu 2020
59080.34 – .39	95	−1.038	0.006	V	Tartu 2020
59081.38 – .43	114	−1.044	0.004	V	Tartu 2020
59112.31 – .36	106	−1.038	0.005	V	Tartu 2020
59115.31 – .42	239	−1.037	0.006	V	Tartu 2020
59120.32 – .42	243	−1.045	0.007	V	Tartu 2020
59123.32 – .47	840			–	Bruneck 2020
59129.23 – .27	85	−1.039	0.006	V	Tartu 2020
59136.26 – .42	749	−1.037	0.009	–	Bruneck 2020
59136.36 – .40	115	−1.042	0.009	V	Tartu 2020
59137.24 – .39	711	−1.035	0.011	–	Bruneck 2020
59141.25 – .35	108	−1.041	0.010	V	Tartu 2020
59141.27 – .40	577	−1.036	0.005	–	Bruneck 2020
59151.22 – .36	624	−1.036	0.007	V	Tartu 2020
59157.18 – .36	822	−1.039	0.007	V	Tartu 2020
59160.25 – .35	548	−1.035	0.006	–	Bruneck 2020
59162.20 – .30	528	−1.038	0.005	V	Tartu 2020

Table 2: Differential magnitudes of the comparison stars and mean error of the averages. The outlying differential magnitude at JD 2 458 812.25 was excluded from the calculation of the mean value for Tartu 2019.

Site	Band	N	C_1–C_2
Bruneck 2019	–	2536	-1.034 ± 0.001
Bruneck 2020	–	2817	-1.039 ± 0.003
Tartu 2019	V	684	-1.024 ± 0.002
Tartu 2020	V	3246	-1.040 ± 0.001

Table 3: Relative weights assigned to the T_{max} derived in this work.

Weight	Data density		Shape of maximum	Comment
1	very low		(ir)regular	
2	medium	+	irregular	
3	high	+	irregular	deviations from smoothness
4	medium	+	regular	
5	high	+	regular	smooth light curve

Table 4: Times of maximum light (HJD − 2400000) of CY Aqr, weight W (see Table 3), and cycle number E. A digital version of this Table is included as file `tmax2019-20.dat`.

T_{max}	W	E	Band	Site
58749.41506	5	533925	V	Tartu 2019
58752.40611	5	533974	V	Tartu 2019
58764.43027	1	534171	V	Tartu 2019
58768.27600	5	534234	–	Bruneck 2019
58768.33708	5	534235	–	Bruneck 2019
58768.39801	3	534236	–	Bruneck 2019
58780.36150	3	534432	–	Bruneck 2019
58782.25377	5	534463	–	Bruneck 2019
58782.31500	5	534464	–	Bruneck 2019
58782.37623	5	534465	–	Bruneck 2019
58783.29158	5	534480	–	Bruneck 2019
58783.35266	3	534481	–	Bruneck 2019
58783.41375	3	534482	–	Bruneck 2019
58786.40445	3	534531	V	Tartu 2019
58812.28482	1	534955	V	Tartu 2019
59072.43040	5	539217	V	Tartu 2020
59079.38899	5	539331	V	Tartu 2020
59080.36555	5	539347	V	Tartu 2020
59081.40321	5	539364	V	Tartu 2020
59112.34983	4	539871	V	Tartu 2020
59115.34048	5	539920	V	Tartu 2020
59115.40168	5	539921	V	Tartu 2020
59120.34568	5	540002	V	Tartu 2020
59120.40676	5	540003	V	Tartu 2020
59123.33641	5	540051	–	Bruneck 2020
59123.39757	5	540052	–	Bruneck 2020
59123.45857	5	540053	–	Bruneck 2020
59129.25726	5	540148	V	Tartu 2020
59136.27701	5	540263	–	Bruneck 2020
59136.33782	5	540264	–	Bruneck 2020
59136.39880	5	540265	–	Bruneck 2020
59136.39899	1	540265	V	Tartu 2020
59137.25330	3	540279	–	Bruneck 2020
59137.31460	5	540280	–	Bruneck 2020
59137.37538	5	540281	–	Bruneck 2020
59141.28195	5	540345	–	Bruneck 2020
59141.28196	5	540345	V	Tartu 2020
59141.34296	5	540346	–	Bruneck 2020
59141.34308	5	540346	V	Tartu 2020
59151.23112	5	540508	V	Tartu 2020
59151.29215	5	540509	V	Tartu 2020
59151.35330	5	540510	V	Tartu 2020
59157.21287	5	540606	V	Tartu 2020
59157.27396	5	540607	V	Tartu 2020
59157.33504	5	540608	V	Tartu 2020
59160.26481	5	540656	–	Bruneck 2020
59160.32584	5	540657	–	Bruneck 2020
59162.21807	5	540688	V	Tartu 2020
59162.27895	5	540689	V	Tartu 2020